

# A Two-Dimensional Detailed Ion Channel Model of Abnormal Cardiac Action Potential Propagation

Niels F. Otani

Case Western Reserve University, Cleveland, OH, U.S.A.

## Abstract

Cardiac action potential propagation is modeled with a two-dimensional simulation that includes full Luo-Rudy (LRd) ion channel dynamics. Preliminary results show that the L-type calcium current is dependent on the curvature of the propagating wavefront, and that, in the case of spiral wave reentry, calcium-induced calcium release exhibits complex temporal behavior including occasional large releases which occur on the boundary of the spiral wave core. The core region also exhibits significantly lower intracellular calcium concentrations. The computer model uses a simple forward Euler method in combination with a variable, multiple. The algorithm thereby allows the desktop modeling of a reasonable size spatial region while simultaneously providing for a detailed representation of the action potential upstroke. Attempts to reduce the runtime of the code, including parallelization issues, are also discussed.

## 1. Introduction

The question of whether various types of cardiac tachycardias and fibrillation are caused by functional reentry in the form of spiral waves has been debated now for many years [1]. While it is well known that many simple models of excitable media support spiral wave patterns of action potential propagation, there has been some question as to whether and in what form spiral waves exist in cardiac tissue, and realistic computer models thereof.

In this paper, we discuss *preliminary* results from our two-dimensional computer model, which employs the Luo-Rudy (LRd) ion channel model as the basis for its local dynamics. This model is currently the most detailed model of the electrical properties of ventricular muscle currently in widespread use.

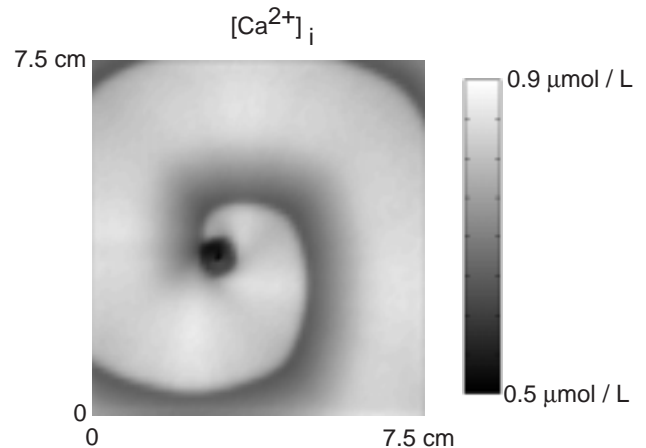


Figure 1. Intracellular calcium concentration in an LRd dynamics spiral wave.

## 2. Numerical Model

The model consists of identical copies of the complete LRd model [2,3] arranged on a two-dimensional rectangular grid, connected to one another through fixed resistances representative of gap-junction resistances. Each copy of the LRd model is advanced in time using the forward Euler method with a variable timestep. The timestep size is determined on the fly by requiring that approximations for the error in  $V$  (the membrane potential) and  $m$  (one of the fast sodium channel gating variables) remain below specified values. The errors are estimated by finite difference versions of the quantities  $(1/2)\Delta t^2(d^2V/dt^2)$  and  $(1/2)\Delta t^2(d^2m/dt^2)$  respectively. If the timestep calculated in this manner is smaller than 90% of its previously calculated value, then it is assumed that the second derivative estimates themselves are not calculated accurately, and the latest estimate of the timestep is used to recalculate them. This process is repeated until the timestep is at least 90% of its previously computed value.

Cells are advanced in order of their current times; that is, the cell which was most backward in time is the next to

be advanced. This is accomplished using a fairly standard binary tree scheduling algorithm as detailed in [4].

The membrane voltages from adjacent grid cells are required to calculate currents through the gap junction resistances. Since each cell has its own timestep, the current times of the cells adjacent to a given cell are generally not the same as that of the given cell. The order of cell updating defined by the binary tree scheduler does, however, guarantee that the current time of any of the adjacent cells follows, and the last previous time of these cells precedes, the current time of the cell to be updated. We therefore obtain membrane voltages from adjacent cells by interpolating from these two times to the current time of the cell to be advanced.

Our first simulations consisted of two types of runs: those with the spatial dimension of the cells much smaller than the space constant, and those with cell dimension of order the space constant. For the former, we used the parameters: cell size: 293  $\mu\text{m}$  by 293  $\mu\text{m}$ , gap junction resistances: 78.92  $\text{M}\Omega / \text{cm}$  in both directions, and a grid size of 256 x 256. For the latter, we used cells of size 1.17 mm by 1.17 mm, gap junction resistances again of 78.92  $\text{M}\Omega / \text{cm}$ , and a grid size of 64 x 64.

Simulations of the first type (with grid size 256 x 256) took approximately 30 hours of CPU time on a 300MHz Sun Ultrasparc II for a 2000 ms run. We made two attempts to improve the runtime of the code:

(1) We tried changing most of the cells into what we called "Vm" cells, which calculated V, m, the sodium current, the time, the timestep, and the gap-junction currents as in the full "LRd" cells, but interpolated all the remaining currents from the closest LRd cells. The latter were much fewer in number and arranged on a coarser grid. The idea is that only the explicitly represented quantities in the Vm cells require fine spatial resolution, so we expected that it would be faster and harmless to interpolate the remaining quantities as needed. Result: some minor differences appeared in the calcium concentrations, while other quantities were fairly accurately represented. The runtime, however, was still 17 hours. The interpolation process itself was found to be the culprit, either because of caching problems, or slow C++ virtual table lookup. Analysis is continuing.

(2) We also tried parallelizing the code with each of 8 threads taking turns advancing the next scheduled cell. This code only ran 10% faster—very disappointing. The problem in this case lies either with the thread locking system, or with the binary tree scheduler as a bottleneck. Again, examination of the problem is ongoing. Parallelization based on domain decomposition may be necessary.

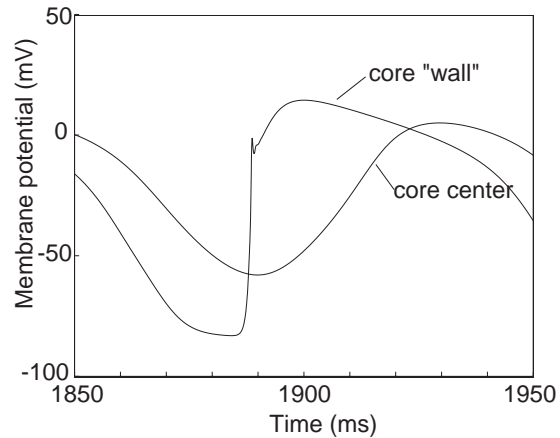


Figure 2. Membrane potentials in the spiral wave core and just outside the core as functions of time. Approximately one spiral wave period is shown.

### 3. Results

We had no trouble creating a spiral wave in our 2-d LRd model. A cross-field stimulation protocol formed the wave. A plane wave action potential is first initiated by depolarizing the bottom edge of the simulation region. When the trailing edge of this action potential wave has propagated roughly halfway across the system, the left half of the system is depolarized. The result is the formation of the spiral wave shown in Fig. 1.

This "LRd" spiral wave is characterized by a central core region with a time-averaged intracellular calcium concentration lower than that of the surrounding region. This feature is evident in Fig. 1, very much resembling the eye of a hurricane. This depressed calcium region exists without the presence of the analogous feature in the membrane potential. When viewed in terms of the membrane potential, the tip of the spiral wave appears to rotate about a point, rather than around a circular core region, as is the case for the "calcium concentration" spiral wave.

The low-calcium core may be explained through a series of events starting with the behavior of the membrane voltage in the core region as a function of time. As shown in Fig. 2, the core voltage always stays above  $-55 \text{ mV}$ , which prevents any participation whatever by the sodium channels. The elevated average value of the membrane potential is caused by electrotonic effects, which force the voltage to reflect the average value of the membrane potential of the region surrounding the core.

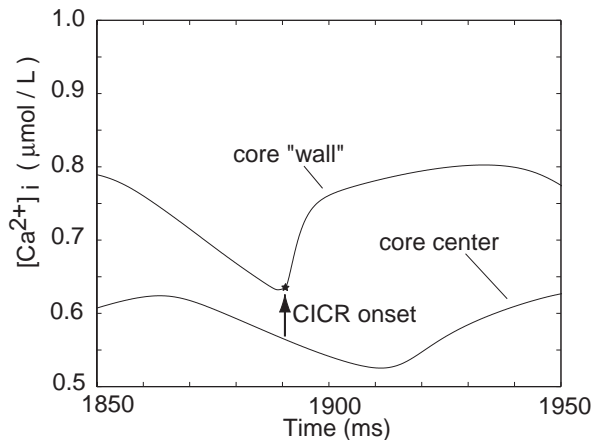


Figure 3. Intracellular calcium in the spiral core, and just outside the core, as functions of time. The arrow shows the point at which calcium-induced calcium release is observed at the observed point in the core wall.

Without sodium current, the time variation of the core membrane potential lacks any identifiable rapid upstroke feature, and in fact looks very nearly sinusoidal in Fig. 2. Contrast this to the membrane potential just outside the core region (which we refer to as the core “wall,” in analogy to the hurricane’s eye wall).

The absence of fast-upstroke action potentials in the core leaves no means by which calcium-induced calcium release (CICR) can be triggered. (CICR requires both a discernible upstroke and an increase in intracellular calcium immediately following the upstroke.) Without CICR, the intracellular calcium in the spiral core oscillates with a smaller amplitude and maintains a lower average value than away from the core (Fig. 3).

These simulations have also produced other results of interest which we yet to analyze in detail. When the cell size is of order the space constant, localized bursts of intracellular calcium sometimes appear on the core wall. This seems to be due to large CICRs, which spring up at irregular intervals when the core wobbles. The spiral wave tip then crosses over cells that had previously been missed. These cells are then capable of the observed large calcium releases.

We also note that, away from the spiral core, the calcium concentration following the passage of the action potential upstroke depends on the curvature of the wavefront. Curiously, in the run in which the cell size is much smaller than the space constant, the highest concentration occurs following that portion of the wavefront with the least curvature. The reverse is true when the cell size is of order the space constant.

## 4. Conclusions

Early results from our two-dimensional, full LRd dynamics simulation model show features that are relevant both to our understanding of general action potential propagation during rapid pacing, and to our understanding of functional reentrant processes such as spiral waves. We demonstrate the usefulness of the model by analyzing one of these features: a low-calcium central core region that develops during spiral wave dynamics. The presence of the underlying LRd ion channel model allows us to explain this feature entirely on the basis of ion channel dynamics, a more satisfying and convincing explanation than one based on a more general model of an excitable medium. In the future, we plan to continue studying features of rapid pacing and spiral wave reentry under both normal and abnormal physiological conditions.

## References

- [1] Winfree, AT. Theory of spirals. In: Cardiac Electrophysiology, from Cell to Bedside, 2nd Edition. DP Zipes and J Jalife, eds. Philadelphia: WB Saunders Press, 1995: 379-389.
- [2] Luo, CH, Rudy, Y. A dynamic model of the cardiac ventricular action potential I. Simulations of ionic currents and concentration changes. *Circulation Research* 1994;74:1071-96.
- [3] Zeng, J, Laurita, KR, Rosenbaum, DS, Rudy Y. Two components of the delayed rectifier  $K^+$  current in ventricular myocytes of the guinea pig type, Theoretical formulation and their role in repolarization. *Circulation Research* 1995; 77:140-52.
- [4] Otani, NF. Computer modeling in cardiac electrophysiology. *Journal of Computational Physics*, submitted.

Address for correspondence.

Niels F. Otani.  
 Department of Biomedical Engineering  
 Case Western Reserve University  
 Cleveland, OH 44106.  
 nfo@po.cwru.edu

